APPENDIX B

9. Matzuk, M. M. *et al. Nature* **374,** 354–356 (1995).
9. Roberts, V. J. & Barth, S. *Endocrinology* **134,** 914–923 (1994).
10. Woodruff, T. K., Lyon, R. J., Hansen, S. E., Rice, G. C. & Mather, J. P. *Endocrinology* **127,** 3196–3205 (1990).
11. Mather, J. P. *et al. Endocrinology* **127,** 3206–3214 (1990).
12. Kaipia, A., Toppari, J., Huhtaniemi, I. & Pranko, J. *Endocrinology* **134,** 2165–2170 (1994).
13. Shikone, T. *et al. Molec. Endocr.* **8,** 963–995 (1994).
14. deWinter, J. P. *et al. Molec. Cell. Endocr.* **83,** R1–R6 (1992).
15. Feng, Z.-M., Madigan, M. B. & Chen, C.-L. C. *Endocrinology* **132,** 2593–2600 (1993).
16. Cameron, V. A. *et al. Endocrinology* **134,** 799–806 (1994).
17. Ritzen, E. M., Hansson, V. & French, F. S. in The Testis 2nd edn (eds Burger, H. & de Kretser, D.) 269–302 (Raven, New York; 1989).
18. Vassali, A. *et al. Genes Dev.* **5,** 414–427 (1994).
19. Hemmati-Brivanlou, A. & Melton, D. A. *Nature* **359,** 609–614 (1992).
20. Hemmati-Brivanlou, A. & Melton, D. A. *Cell* **77,** 273–281 (1994).
21. Schulte-Merker, S., Smith, J. C. & Dale, L. *EMBO J.* **13,** 3533–3541 (1994).
22. Matzuk, M. M. & Bradley, A. *Biochem. Biophys. Res. Commun.* **184,** 404–413 (1992).
23. Matzuk, M. M., Finegold, M. J., Su, J.-G. J., Hsueh, A. J. W. & Bradley, A. *Nature* **360,** 313–319 (1992).
24. Mathews, L. S. & Vale, W. W. *Cell* **65,** 973–982 (1991).
25. Bradley, A. in *Teratocarcinomas and Embryonic Stem Cells: A Practical Approach* (ed. Robinson, E. J.) 113–151 (IRL, Oxford, 1987).
26. Ramirez-Solis, R. *et al. Analyt. Biochem.* **201,** 331–335 (1992).
27. Ramirez-Solis, R. *et al. Cell* **83,** 279–294 (1993).
28. Kumar, T. R., Fairchild-Huntress, V. & Low, M. *Molec. Endocr.* **6,** 81–90 (1992).

ACKNOWLEDGEMENTS. We thank J. van den Eijnden-van Raaij for sharing activin-receptor expression data and other information before publication; N. Lu and R. Towns for technical assistance; C. McDonnell for help with cryostat sectioning; S. Topouzis for help with northern blot analysis; S. Baker and B. Powell for help with manuscript preparation; and R. Behringer and M. Meistrich for advice and review of the manuscript. FSH radioimmunoassay reagents were a gift from the National Hormone and Pituitary Distribution Program, National Institute of Diabetes and Digestive and Kidney Diseases. This research was supported in part by grants (to M.M.M.) from the NIH and the Lalor Foundation. A.B. is an Investigator with the Howard Hughes Medical Institute.

Multiple defects and perinatal death in mice deficient in follistatin

Martin M. Matzuk*†‡, Nalfang Lu†, Hannes Vogel†, Klaus Sellheyer‡, Dennis R. Roop‡ & Allan Bradley*§

Departments of * Molecular and Human Genetics, † Pathology, ‡ Cell Biology, § Howard Hughes Medical Institute, Baylor College of Medicine, Houston, Texas 77030, USA

FOLLISTATIN, an activin-binding protein and activin antagonist *in vitro*[1,2], can bind to heparan sulphate proteoglycans[3] and may function *in vivo* to present activins to their receptors. In the mouse, follistatin messenger RNA is first detected in the deciduum (on embryonic day 5.5), and later in the developing hindbrain, somites, vibrissae, teeth, epidermis and muscle[4–11]. In *Xenopus laevis*, overexpression of follistatin leads to induction of neural tissue[12]. Here we use loss-of-function mutant mice to investigate the function of follistatin in mammals. We find that follistatin-deficient mice are retarded in their growth, have decreased mass of the diaphragm and intercostal muscles, shiny taut skin, skeletal defects of the hard palate and the thirteenth pair of ribs, their whisker and tooth development is abnormal, they fail to breathe, and die within hours of birth. These defects are more widespread than those seen in activin-deficient mutant mice, indicating that follistatin may modulate the actions of several members of the transforming growth factor-β family.

To define the roles of follistatin in mammalian development, a targeted deletion (fs^{nl}) of the 6-exon follistatin gene was generated using embryonic stem (ES) cell technology (Fig. 1*a*), and mice heterozygous for this deletion ($fs^{nl}/+$) were intercrossed to generate mice homozygous for the deleted follistatin allele (fs^{nl}/fs^{nl}). Genotyping of mice at birth and at embryonic day 18.5 (E18.5) revealed that fs^{nl}/fs^{nl} mice (follistatin-deficient) could survive to birth but died within hours of delivery (Fig. 1*b*). Of 196 pups at E18.5, 44 were homozygotes (22.4%), 97 were heterozygote (49.5%) and 55 were wild-type (28.1%), consistent with the expected mendelian frequency of 1:2:1. Low-

FIG. 1 Targeted deletion of the follistatin gene in ES cells and Southern blot analysis of DNA from offspring derived from heterozygous matings. *a*, The targeting vector contains 3.8 kb of isogenic DNA homologous to the 5′ non-translated sequence of the mouse follistatin gene, 3.4 kb of sequence homologous to the 3′ end of the mouse follistatin gene, a PGK–*hprt* (where PGK represents phosphoglycerate kinase I promoter) expression cassette, and an MC1-tk (thymidine kinase) expression cassette. Homologous recombination between this targeting vector and the endogenous follistatin gene in mouse ES cells should result in a 5.1-kb deletion of the 6 exons coding for follistatin, ensuring that no follistatin mRNA and therefore no follistatin protein was produced in animals homozygous for the targeted allele. Introduction of new diagnostic restriction endonuclease sites (*BglII* and *XbaI*) were used to differentiate wild-type versus recombinant alleles. Six ES cell clones out of 1,290 clones (1:215) screened by Southern blot analysis[21,22] were correctly targeted. One ES cell clone, FS3-C2, gave rise to multiple male chimeras and germline transmission of the deleted allele was demonstrated for 3 of 4 chimaeric males. Male and female mice heterozygous for the deleted follistatin allele occurred at the expected ratio and were viable and fertile. *b*, Genomic (tail) DNA (~5 μg) from offspring from a single litter was restricted with *XbaI* and *EcoRI* and analysed by Southern blot analysis[21] using a 3′ probe as shown. The presence of a 5.9-kb fragment versus a 3.7-kb wild-type fragment is diagnostic of the deletion when using the 3′ probe. Homozygote offspring are dead within hours of birth. WT, wild type; +/−, heterozygote; −/−, homozygote mutant. *c*, Southern blots of wild-type (WT) and fs^{nl}/fs^{nl} (−/−) mice, chicken and *Xenopus laevis* genomic DNA (5 μg per lane) digested with *BamHI* were analysed using a human follistatin cDNA. The absence of any hybridizable fragment bands in the lane genotyped as homozygote (−/−) confirmed that these mice lack the 6 exons coding for the follistatin gene, that this is a null allele (fs^{nl}), and that there were no follistatin-related genes in the mouse.

METHODS. More than 20 kb of DNA encompassing the 6-exon mouse follistatin gene sequences was isolated from a 129SvEv genomic library using a follistatin cDNA. Linearized vector (25 μg) was electroporated into the *hprt*-negative AB2.1 ES cell line, selected in HAT and FIAU (where HAT represents hypoxanthine, aminopterin, thymidine, and FIAU is (1-(2′-deoxy-2′-fluoro-β-D-arabinofuranosyl)-5-iodouracil), and clones were injected into blastocysts to generate chimaeras[21]. Enrichment in HAT and FIAU was 32-fold compared to HAT alone. Southern blot analysis of the ES cell clones was as described[21,22]. Low-stringency hybridization of the mouse, chicken and *Xenopus laevis* blot was by overnight hybridization at 60 °C followed by 4 washes for 30′ each at 50 °C with a 2 × SSC, 1% SDS solution.

stringency hybridization with a follistatin complementary DNA could detect genomic fragments in wild-type mouse, chicken and *Xenopus laevis* but not in the fs^{nl}/fs^{nl} mice, confirming that we had deleted the only follistatin gene present in the mouse (Fig. 1*c*).

fs^{nl}/fs^{nl} newborns could be phenotypically scored because they were growth-retarded and had shiny, taut skin similar to that seen in the human condition of restrictive dermopathy[13] (Fig. 2*a*). The phenotypic effects of follistatin deficiency were independent of the genetic background (that is, the phenotype was similar on 129SvEv inbred, C57/129 hybrid and C57B1/6 (3 backcrosses) genetic backgrounds). At birth, most fs^{nl}/fs^{nl} mice remained pale and cyanotic, the lungs of the fs^{nl}/fs^{nl} mice sank in liquid and, on histological examination, the alveolar spaces were poorly expanded, consistent with poor breathing, although primary pulmonary defects could not be detected (data not shown). Analysis of the central and peripheral nervous system by gross dissection and histological procedures did not detect any significant abnormalities. Immunohistochemistry of E10.5 whole-mount embryos using an antibody raised against the 155K neurofilament protein[14] indicated that cranial nerves V, VII, IX and X and the spinal ganglia were developing normally (data not shown).

Defects were detected in the musculoskeletal system. fs^{nl}/fs^{nl} mice lacked incisors (6 of 34, hybrid background; Fig. 2*b*) or had delayed incisor development (Table 1). Three of 19 (16%) hybrid background fs^{nl}/fs^{nl} mice had a cleft secondary palate. Six out of 11 129SvEv inbred mice (55%) and 6 out of 28 C57/

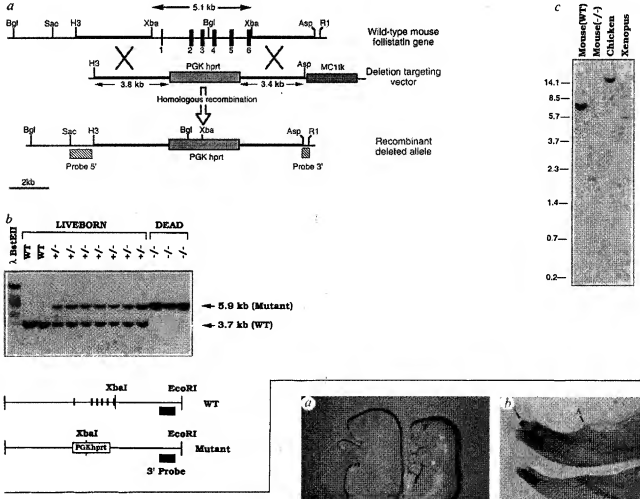

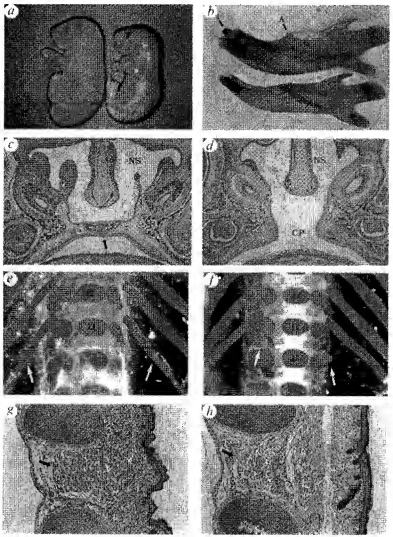

FIG. 2 Morphological and histological analysis of follistatin and control mice. *a*, Control (left) and fs^{m1}/fs^{m1} (right) newborn mice. The fs^{m1}/fs^{m1} mouse on the right was smaller, hypoxic (pale), and had shiny, taut skin compared to the control. Weighing of pups at E18.5 revealed that homozygotes (1.04 ± 0.10 g; $n = 30$) were ~12% lighter than their heterozygote (1.18 ± 0.10 g; $n = 52$) and wild-type (1.17 ± 0.13 g; $n = 18$) littermates. *b*, Medial view of wild-type (top) and fs^{m1}/fs^{m1} (bottom) dissected mandibles stained with alizarin red and alcian blue as described[23]. The alveolar ridge (A), the region of the mandible that surrounds the lower molars, is less prominent and the incisor (I) is missing in the mutant. *c* and *d*, Coronel sections of the head were made at the level of the eye of wild-type (*c*) and fs^{m1}/fs^{m1} (*d*) mice and the sections stained with alcian blue and neutral red. There is a cleft palate (CP) in the fs^{m1}/fs^{m1} mouse (*d*). The oral cavity is contiguous with the nasal sinus (NS) in *d*. The arrow points to the normal palate in *c*. *e* and *f*, Skeletal analysis (alizarin red stain) of the thirteenth pair of ribs from control (*e*) and fs^{m1}/fs^{m1} mutant (*f*) mice. The thirteenth pair of ribs is either absent or limited in its formation (arrows, *f*) compared to the same pair in the control (arrows, *e*). Thoracic vertebral bodies are numbered for orientation. *g* and *h*, Analysis of the intercostal (arrows) and pectoralis major musculature from wild-type (*g*) and fs^{m1}/fs^{m1} (*h*) mice taken at the same level (between ribs 3 and 4). Note that the muscle fibres from the mutant are more sparse and less full than the control. A comparable situation is seen in the diaphragm (data not shown).

129 hybrid genetic background mice (21%) lacked a hard palate similar to activin-βA-deficient mice[13] (see below; Fig. 2*c*, *d*). Both inbred and hybrid fs^{ml}/fs^{ml} mice had defects in the thirteenth pair of ribs and a decrease in the number of lumbar vertebrae (Fig. 2*e*, *f*; Table 1). The size of the ribs and penetrance of this phenotype was dependent on the genetic background (Table 1). The intercostal (Fig. 2*g*, *h*) and diaphragmatic (data not shown) muscles showed a decrease in muscle mass consistent with expression of follistatin in the muscle at birth[10]. Histological and electron microscope analysis of the musculature, including analysis of ATPase activity, glycogen content and mitochondria, failed to demonstrate any primary defect (data not shown). Thus, it is not clear whether the decrease in muscle mass in the fs^{ml}/fs^{ml} mice is primary or secondary to an overall growth deficiency.

Whisker development was abnormal: the whiskers were too thin and were inappropriately oriented, suggesting that follistatin may be an important modulator of activin-βA action (Fig. 3*a–d*; see accompanying Letter). The skin showed hyperkeratosis, as indicated by thickened granular and stratum corneum layers (Fig. 3*e*, *f*). Electron microscope examination revealed a 25% increase in the stratum corneum cells compared to controls. The shiny, taut skin of fs^{ml}/fs^{ml} mice (Fig. 2*a*) resembles the skin of transgenic mice with directed overexpression of transforming growth factor (TGF)-β1 to the epidermis using a human keratin-1 promoter (HK1.TGF-β1)[16]. Keratin-6 expression was abnormal in the interfollicular epidermis of the fs^{ml}/fs^{ml} mice, as it was in HK1.TGF-β1 mice (Fig. 3*h*). Normally keratin-6 is found only in the outer root sheath of hair follicles (Fig. 3*g*). Although abnormal keratin-6 expression is often associated with hyperproliferation[17], the fs^{ml}/fs^{ml} mice showed normal epidermal mitotic activity as judged by 5-bromodeoxyuridine labelling. These results, together with those obtained for the growth-arrested epidermis of HK1.TGF-β1 mice[16], suggest that keratin-6 expression can occur in response to a variety of stimuli that perturb normal epidermal development.

In conclusion, fs^{ml}/fs^{ml} mice have defects in the musculoskeletal system and in the epidermis, and this constriction effect probably contributes to their rapid demise. Follistatin is expressed in the rhombomeres in the mid-gestational mouse[2], and can cause differentiation of neural cell lines[18]; overexpression in *Xenopus laevis* suggests that follistatin may be essential for neural induction[12]. Our results show that the absence of follistatin in the mouse *in vivo* does not apparently affect the gross development of the nervous system. Interestingly, the fs^{ml}/fs^{ml} mice demonstrate abnormal whisker and tooth development and hard-palate defects similar to activin-βA-deficient mice[13]. In the vibrissae, teeth and palate, where follistatin is expressed adjacent to activin-βA[7], follistatin appears to play a role in activin signal transduction, possibly sequestering activins in heparan sulphate proteoglycans[7] and presenting activin to activin receptors similar to type III TGF-β receptors[19]. The follistatin-deficient mice also have other defects not seen in activin-deficient mice[13]. Some of these defects are similar to those of the BMP-5 (*short ear*) mutant mice, which have defects in the thirteenth pair of ribs[20], and the TGF-β overexpressors, which have shiny, taut skin[16]. These

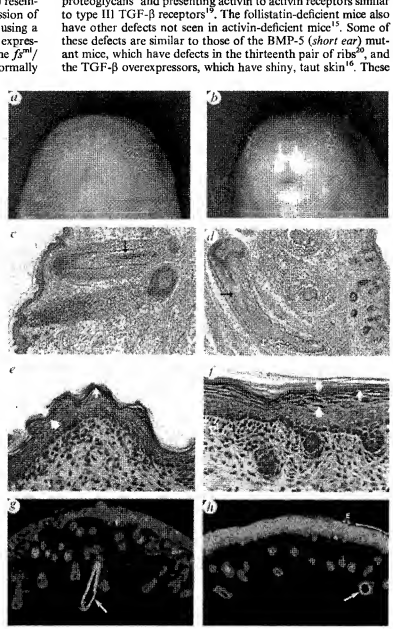

FIG. 3 *a* and *b*, Gross analysis of the whisker pads and face of control (*a*) and fs^{ml}/fs^{ml} (*b*) newborn mice demonstrating the disoriented whiskers and shiny skin of the mutant (*b*). c and *d*, Histological analysis (haematoxylin and eosin stain of transverse sections) of the whisker follicles of control (*c*) and fs^{ml}/fs^{ml} (*d*) newborn mice. The whisker shafts (arrow) are perpendicular to the surface in the control (*c*). In the mutant (*d*), the shaft (arrow) projects parallel before turning perpendicularly. e and f, Histology of the skin of control (e) and fs^{ml}/fs^{ml} (*f*) newborn mice photographed at the same magnification. Note the thickened granular (between large white arrows, left) and stratum corneum (between small white arrows, right) layes in the mutant (*f*) compared to the control (e). *g* and *h*, Double-label immunofluorescence of the skin from the back of E18.5 control (*g*) and fs^{ml}/fs^{ml} (*h*) mice. The antibody raised against keratin 14 (red) will stain both interfollicular epidermis and hair follicle, whereas the antibody against keratin 6 (yellow/green) will normally stain only the outer root sheath (arrow) of the hair follicle (*g*). In the mutant (*h*), abnormal keratin 6 expression seen in the interfollicular epidermis (E). Single-label immunofluorescence of the mutant skin did not reveal any abnormality in keratin 14 expression (data not shown).
METHODS. Histological analysis of the muscle and skeleton, and double-label immunofluorescence of the skin were performed as described[18,21,23].

TABLE 1 Skeletal, palate and tooth defects

	13th pair of ribs		Five lumbar	Palate defects		Lower incisors	
	Intact	Anlage	Zero ribs	vertebrae*	Cleft	Hard palate	Absent	Delayed
C57/129 hybrid								
Wild-type	15	0	0	2/15	0	0	0	0
Heterozygote	29	6	0	21/35	0	0	0	0
Homozygote†	3	17	8	28/28	3/19	6/28	6/34	23/34
129 inbred								
Wild-type	9	0	0	0/9		0	0	0
Heterozygote	11	4	0	13/15		0	0	0
Homozygote	0	9	2	11/11		6/11	0/11	11/11

* Six lumbar vertebrae are the normal complement in the mouse.
† In 4/28 homozygotes, one or both of the seventh ribs failed to fuse to the sternum.

similarities suggest that follistatin may be a modulator of other TGF-β-related proteins or may function independently. Thus, the results obtained by overexpression of follistatin in *Xenopus laevis*[15] may be a consequence of up or downregulation of the actions of several TGF-β-related proteins. It will be critical to compare mice deficient in other TGF-β superfamily members to our follistatin-deficient mice in order to establish the extent to which follistatin is involved in signal transduction of other TGF-β-related protcins. □

Received 9 November 1994; accepted 24 January 1995.

1. Michel, V., Farnworth, P. & Findlay, J. K. *Molec. cell. Endocr.* **91,** 1–11 (1993).
2. Nakamura, T. *et al. Science* **247,** 836–838 (1990).
3. Nakamura, T., Sugino, K., Titani, K. & Sugino, H. *J. biol. Chem.* **266,** 19432–19437 (1991).
4. van den Eijnden-van Raalj, A. J. M., Feijen, A., Lawson, K. A. & Mummery, C. L. *Devl Biol.* **154,** 356–365 (1992).
5. Albano, R. M., Arkell, R., Beddington, R. S. P. & Smith, J. C. *Development* **120,** 803–813 (1994).
6. Feijen, A., Goumans, M. J. & van den Eijnden-van Raalj, A. J. M. *Development* **120,** 3621–3637 (1994).
7. Roberts, V. J. & Barth, S. *Endocrinology* **134,** 914–923 (1994).
8. Shimasaki, S. *et al. Mol. Endocrinology* **3,** 652–659 (1989).
9. Michel, V., Albiston, A. & Findlay, J. K. *Biochem. biophys. Res. Commun.* **173,** 401–407 (1990).
10. Michel, V., Rao, A. & Findlay, J. K. *Biochem. biophys. Res. Commun.* **180,** 223–230 (1991).
11. Tashiro, K. *et al. Biochem. Biophys. Res. Commun.* **174,** 1022–1027 (1991).
12. Hemmati-Brivanlou, A., Kelly, O. G. & Melton, D. A. *Cell* **77,** 283–295 (1994).
13. Pierard-Franchimont, C. *et al. J. Path.* **167,** 2223–2228 (1992).
14. Chiseka, O., Musci, T. S. & Capecchi, M. R. *Nature* **335,** 516–520 (1992).
15. Matzuk, M. M. *et al. Nature* **374,** 354–356 (1995).
16. Seilheyer, K. *et al. Proc. natn. Acad. Sci. U.S.A.* **90,** 5237–5241 (1993).
17. Weiss, R. A., Eichner, R. & Sun, T.-T. *J. Cell Biol.* **98,** 1397–1406 (1984).
18. Hashimoto, M. *et al. J. biol. Chem.* **267,** 7203–7206 (1992).
19. Lopez-Casillas, F., Wrana, J. L. & Massague, J. *Cell* **73,** 1435–1444 (1993).
20. Kingsley, D. M. *et al. Cell* **71,** 399–410 (1992).
21. Matzuk, M. M., Finegold, M. J., Su, J-G. J., Hsueh, A. J. W. & Bradley, A. *Nature* **360,** 313–319 (1992).
22. Ramirez-Solis, R. *et al. Analyt. Biochem.* **201,** 331–335 (1992).
23. Ramirez-Solis, R. *et al. Cell* **83,** 279–294 (1993).

ACKNOWLEDGEMENTS. We thank S. Baker and B. Powell for assistance with manuscript preparation; W. Moyle and R. Myers for their help in isolating follistatin cDNA; R. Behringer, J. Bickenbach and T. Rajendra Kumar for critically reviewing the manuscript; and J. Bickenbach for advice on histology and electron microscopy. This research was supported in part by grants from the NIH (to M.M.M.). A.B. is an associate investigator with the Howard Hughes Medical Institute.

The product of *hedgehog* autoproteolytic cleavage active in local and long-range signalling

Jeffery A. Porter, Doris P. von Kessler, Stephen C. Ekker, Keith E. Young, John J. Lee, Kevin Moses* & Philip A. Beachy

Howard Hughes Medical Institute, Department of Molecular Biology and Genetics, The Johns Hopkins University School of Medicine, Baltimore, Maryland 21205, USA
* Department of Biological Sciences, University of Southern California, Los Angeles, California 90089, USA

THE secreted protein products of the *hedgehog* (*hh*) gene family are associated with local and long-range signalling activities that are responsible for developmental patterning in multiple systems, including *Drosophila* embryonic and larval tissues[1–4] and vertebrate neural tube, limbs and somites[5–15], in a process that is critical for full biological activity, the *hedgehog* protein (Hh) undergoes autoproteolysis to generate two biochemically distinct products, an 18K amino-terminal fragment, N, and a 25K carboxy-terminal fragment, C (ref. 16); mutations that block autoproteolysis impair Hh function. We have identified the site of autoproteolytic cleavage and find that it is broadly conserved throughout the *hedgehog* family. Knowing the site of cleavage, we were able to test the function of the N and C cleavage products in *Drosophila* assays. We show here that the N product is the active species in both local and long-range signalling. Consistent with this, all twelve mapped *hedgehog* mutations either affected the structure of the N product directly or otherwise blocked the release of N from the Hh precursor as a result of deletion or alteration of sequences in the C domain.

To characterize the signalling molecules produced from the uncleaved Hh precursor U, we determined the site of autoproteolysis and the structures of the cleaved products using a purified Hh protein from a bacterial source. This purified protein, His_6C, contains primarily carboxy-terminal sequences and can generate a 25K cleavage product corresponding to the native C cleavage product produced in *Drosophila* cells (Fig. 1*a*). In reactions lasting 3 h and using a wide range of concentrations of starting material, this protein displayed kinetics that were independent of concentration, strongly suggesting that the cleavage was intramolecular (Fig. 1*b*).

Amino-terminal sequencing of the 25K cleavage product showed that Hh is cut between Gly 257 and Cys 258 (Fig. 1*c*). Sequence alignment with other insect and vertebrate *hh* proteins demonstrates the absolute conservation of the Gly-Cys-Phe sequence at the site of autoproteolysis (Fig. 1*d*). To test for the presence of a cysteine residue at the amino terminus of C fragments derived from *Drosophila* (*hh*), zebrafish (*twhh* and *shh*) (S.C.E., manuscript submitted) and mouse (*shh*) genes, ^{35}S-cysteine was incorporated during *in vitro* translation (Fig. 1*e*). Figure 1*f* shows that the first round of protein sequencing in each case released the proportion of total incorporated ^{35}S corresponding to a single cysteine residue, establishing that cysteine